Prolonged antigen survival and cytosolic export in cross-presenting human γδ T cells

Simone Meuter[1], Matthias Eberl, and Bernhard Moser[2]

Department of Infection, Immunity and Biochemistry, School of Medicine, Cardiff University, Cardiff CF14 4XN, United Kingdom

Edited* by Peter Cresswell, Yale University School of Medicine, New Haven, CT, and approved March 30, 2010 (received for review March 3, 2010)

Human blood Vγ9Vδ2 T cells respond to signals from microbes and tumors and subsequently differentiate into professional antigen-presenting cells (γδ T-APCs) for induction of $CD4^+$ and $CD8^+$ T cell responses. γδ T-APCs readily take up and degrade exogenous soluble protein for peptide loading on MHC I, in a process termed antigen cross-presentation. The mechanisms underlying antigen cross-presentation are ill-defined, most notably in human dendritic cells (DCs), and no study has addressed this process in γδ T-APCs. Here we show that intracellular protein degradation and endosomal acidification were significantly delayed in γδ T-APCs compared with human monocyte-derived DCs (moDCs). Such conditions are known to favor antigen cross-presentation. In both γδ T-APCs and moDCs, internalized antigen was transported across insulin-regulated aminopeptidase (IRAP)–positive early and late endosomes; however, and in contrast to various human DC subsets, γδ T-APCs efficiently translocated soluble antigen into the cytosol for processing via the cytosolic proteasome-dependent cross-presentation pathway. Of note, γδ T-APCs cross-presented influenza antigen derived from virus-infected cells and from free virus particles. The robust cross-presentation capability appears to be a hallmark of γδ T-APCs and underscores their potential application in cellular immunotherapy.

antigen cross-presentation | dendritic cells | γ/δ T cells | influenza virus

Immunity to intracellular pathogens and tumors is dependent on MHC I–restricted cytotoxic $CD8^+$ T cells (CTLs), which kill infected and transformed cells. The conventional MHC I pathway involves the processing and presentation of endogenous antigen, thereby marking infected tissue cells and tumors as targets for CTLs. However, many viruses do not infect antigen-presenting cells (APCs), and most tumors do not arise in APCs. In these instances, protective immunity fully depends on MHC I loading of peptides from exogenous antigen, an ill-defined process known as antigen cross-presentation (1–4). Although there is consensus that lymphoid tissue resident $CD8^+$ DCs are the main cross-presenting DC subset in mice (2, 3), much less is known about their human counterpart. Recent evidence suggests that human plasmacytoid DCs may fulfill this function, but this finding is a matter of debate (5–8). Because of restricted tissue access, most human studies have focused on in vitro–generated monocyte-derived DCs (moDCs), which have excellent phagocytic activity but limited ability to cross-present soluble antigen (7, 9–11).

We and others recently reported that activated human Vγ9Vδ2 T cells (γδ T-APCs) are a distinct type of professional APCs (10, 12–14). Vγ9Vδ2 T cells represent the major subset of γδ T cells in human peripheral blood that differ from their αβ T cell counterparts in their MHC-independent recognition of small nonpeptide compounds (15–18). Most Vγ9Vδ2 T cells are memory cells with selectivity for microbial-derived (*E*)-4-hydroxy-3-methyl-but-2-enyl pyrophosphate (HMB-PP), explaining their tremendous expansion at early stages of microbial infections (16, 18). Of interest, this antigen selectivity is unique to humans and primates; that is, mouse γδ T cells do not respond to these ligands. Activation of Vγ9Vδ2 T cells leads to rapid production of proinflammatory cytokines and target cell killing (15–18). In addition, activated Vγ9Vδ2 T cells express many features of APCs, including adhesion receptors, costimulatory molecules, and classical (MHC I and II) antigen-presenting molecules, and are highly effective APCs in vitro for both memory and naïve αβ T cells (12, 18). Of note, and in contrast to moDCs, we demonstrated that γδ T-APCs efficiently cross-present soluble protein (10). γδ T-APCs and moDCs did not differ in their ability to induce $CD4^+$ T cell responses or to present peptides to $CD8^+$ T cells, indicating main differences in their antigen cross-presentation pathway(s).

The molecular mechanisms underlying cross-presentation in γδ T-APCs are unknown but may involve a specialized "cross-presentation machinery" similar to that in mouse $CD8^+$ DCs (2, 3). Critical factors for cross-presentation are (*i*) route of antigen uptake, (*ii*) acidification sensitive antigen degradation in endosomes/lysosomes, and (*iii*) antigen entry into the MHC I pathway (1, 2). The canonical cytosolic pathway involves the translocation of endocytosed antigen into the cytosol, followed by its degradation by the proteasome and processing by the MHC I loading complex in the endoplasmic reticulum (ER). An alternative and less well-defined pathway is the endosomal or vacuolar pathway, with antigen degradation and MHC I loading occurring in endosomes/phagosomes (1, 2). Although the in vivo relevance of these pathways is unknown, the cytosolic pathway is generally considered the more relevant (2).

Based on the essential role for cross-presentation in the control of infections and tumors, we examined the molecular mechanisms that allow γδ T-APCs to process exogenous antigen for the induction of human $CD8^+$ T cell responses. We report unexpected differences between γδ T-APCs and moDCs in their intracellular antigen routing and degradation. In fact, our findings reveal a highly efficient cross-presentation pathway in γδ T-APCs that involves the cytosolic route of MHC I loading. Antigen cross-presentation by γδ T-APCs was not restricted to soluble protein, but included cellular debris and virus particles, underscoring their potential use in immunotherapy.

Results

Delayed Endosomal Acidification and Proteolysis in γδ T-APCs. We reported previously that γδ T-APCs outperform human moDCs in the cross-presentation of soluble protein (10). The reason for this difference is unknown but might involve differences in antigen uptake and/or processing. We first analyzed the endocytic activity of γδ T-APCs using different soluble substrates (BSA, dextran, and Lucifer yellow). Whereas immature DCs are known for their high level of endocytosis, γδ T-APCs showed diminished endocytic activity that did not differ substantially from that of human αβ T cells, B cells, and monocytes (Fig. S1*A*). Thus, the efficiency of cross-presentation did not correlate with antigen uptake, which agrees with recent findings in

Author contributions: S.M., M.E., and B.M. designed research; S.M. and M.E. performed research; S.M., M.E., and B.M. analyzed data; and S.M., M.E., and B.M. wrote the paper.

The authors declare no conflict of interest.

*This Direct Submission article had a prearranged editor.

[1]Present address: Immunology Division, The Walter and Eliza Hall Institute of Medical Research, Parkville, Victoria 3050, Australia.

[2]To whom correspondence should be addressed. E-mail: moserb@cardiff.ac.uk.

This article contains supporting information online at www.pnas.org/lookup/suppl/doi:10.1073/pnas.1002769107/-/DCSupplemental.

DCs (9, 19). We further studied the mechanism of endocytosis using dimethyl amiloride (DMA), a Na^+/H^+ channel inhibitor that selectively blocks macropinocytosis, and cytochalasin D, which inhibits phagocytosis by preventing actin polymerization. Although both inhibitors blocked endocytosis in moDCs, only DMA inhibited the uptake of BSA in γδ T-APCs, indicating that cytoskeleton rearrangement was not involved in the uptake of soluble antigen by γδ T-APCs (Fig. S1*B*). Intracellular processing of endocytosed antigen is a critical next step in cross-presentation (20). Whereas fast degradation was shown to prevent cross-presentation, a delay in lysosomal proteolysis increased its efficiency (20, 21). In support of this finding, initial endosomal alkalinization followed by slow acidification was reported to promote cross-presentation (22). Collectively, diminished lysosomal activity is thought to allow antigen "escape" into the cytosol for processing by the cross-presentation machinery and induction of CTL responses.

To examine antigen degradation, we pulsed γδ T-APCs and moDCs with FITC-BSA, followed by a 0.5 to 6 h chase and analysis by flow cytometry (FACS). Surprisingly, after a 6 h chase, γδ T-APCs still emitted the same level of fluorescence as after the pulse (0 h chase) (Fig. 1*A*). In contrast, moDCs lost >75% of their fluorescence within 3 h and >95% within 6 h. This phenomenon was observed in fresh and activated γδ T cells, whereas fluorescent signals were decreased by ≥50% in αβ T cells, B cells, and monocytes after a 6 h chase (Fig. S2*A*). Rapid loss of the FITC signal in moDCs could have been due to degradation/excretion and/or antigen sequestration in acidic compartments. When we pulsed moDCs with BSA coupled to the pH-insensitive fluorochrome Alexa Fluor 488, we observed full maintenance of the fluorescence over a 24 h chase period (Fig. S2*B*), demonstrating that rapid fluorescence quenching was the cause of the observed loss of the FITC signal. To corroborate this conclusion, we measured the pH in BSA-containing endosomes. Whereas the pH in moDCs dropped from 7 to 4.5 during the 3 h chase period, γδ T-APCs maintained a neutral pH (Fig. 1*C*), indicating that most of the antigen in γδ T-APCs did not access acidic compartments (pH < 5.5) within the first 6 h. In DCs, the NADPH oxidase NOX2 has been shown to control endosomal pH (22); however, using a NOX2-specific inhibitor, we found no evidence of NOX2 involvement in pH control in γδ T-APCs (Fig S3). To determine whether the slow endosomal acidification in γδ T-APCs affected lysosomal proteolysis, we assessed BSA degradation by Western blot analysis. Whereas moDCs degraded most of the BSA within 3 h, γδ T-APCs exhibited a significant delay in proteolysis (Fig. 1*C*). We conclude that γδ T-APCs and moDCs differ fundamentally in terms of the kinetics of endosomal acidification and protein degradation.

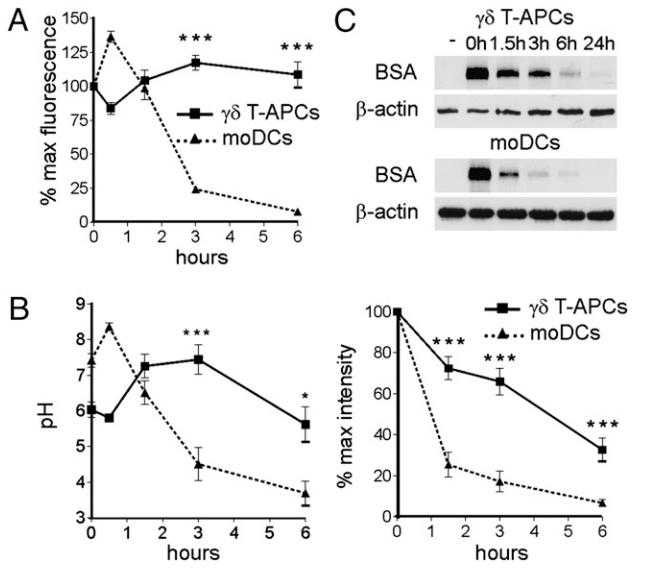

Fig. 1. γδ T-APCs delay endosomal acidification and antigen proteolysis compared with moDCs. (*A*) Residual fluorescence of FITC-BSA–pulsed γδ T-APCs and moDCs over a 6 h chase period. Values were calculated as percentage of maximal fluorescence after the pulse and expressed as mean ± SEM (n = 8–10). (*B*) Kinetics of endosomal pH in γδ T-APCs and moDCs, expressed as mean ± SEM of four independent experiments. (*C*) Western blot analysis of protein degradation in FITC-BSA–pulsed γδ T-APCs and moDCs (top), and quantification of residual protein expressed as percentage of maximal intensity after the pulse (mean ± SEM, n = 6–8) (bottom). *P < 0.05; **P < 0.01; ***P < 0.005.

Traffic of Internalized Antigen in γδ T-APCs and moDCs. The cellular compartments involved in cross-presentation in γδ T-APCs are unknown. While the importance of the cytosolic pathway is widely accepted, the presence of vesicular compartments mediating cross-presentation (e.g. ER–phagosome fusion compartment or recycling endosomes) remains controversial (2, 5, 23). We examined the fate of endocytosed protein by confocal microscopy in γδ T-APCs and moDCs after a 1 h pulse (Fig. 2) and after a 1.5 h chase (Fig. S4). As expected, in the majority of cells (60% of γδ T-APCs and 100% of moDCs), during the pulse, BSA initially colocalized with the early endosomal marker EEA-1 (Fig. S5). Within individual positive cells (>0% colocalization in Fig. S5*B*), only 30% of endocytosed BSA colocalized with EEA-1 in both APCs, possibly reflecting the dynamic process of endocytosis. After a subsequent chase period, this colocalization was lost in all cells analyzed, indicating that the internalized protein had left early endosomes. In >60% of both APCs, BSA was found to partially colocalize (21%–27%) with the late endosomal/lysosomal marker Lamp-1. Surprisingly, in all cells analyzed, a major fraction of BSA-containing vesicles was not associated with Lamp-1, even after the chase period; thus, we investigated whether BSA might have traveled to recycling endosomes, a compartment recently proposed to be involved in cross-presentation (5). No colocalization with $rab11^+$ recycling endosomes was identified in γδ T-APCs or moDCs, however. Similarly, preliminary experiments in γδ T-APCs revealed no BSA colocalization with the ER marker calnexin. Although these experiments cannot prove that antigen does not traffic through these compartments in γδ T-APCs at any given time point, they certainly cannot account for the antigen-containing Lamp-1–negative vesicles.

Of interest, early after endocytosis we detected substantial colocalization of BSA with the insulin-regulated aminopeptidase (IRAP) in the majority (>80%) of γδ T-APCs and moDCs (colocalization of 22% and 44%, respectively). IRAP is a peptide-trimming peptidase suggested to be involved in proteasome-dependent cross-presentation and found in early endosomes (24). After the 1.5 h chase, this colocalization was lost in 40% of γδ T-APCs and in all moDCs. In conclusion, our data indicate that in both APCs, internalized soluble protein travels from early to late endosomal or lysosomal compartments, with no substantial contribution of recycling endosomes.

Cytosolic Export and Processing. Because we found no distinct vesicular compartments in support of the endosomal/vacuolar pathway in γδ T-APCs, we turned our attention to the cytosolic pathway. The fundamental step in this model is the translocation of internalized antigen from endosomes to the cytosol for degradation by the proteasome (1–4). To directly analyze antigen translocation, we used the recently described model of cytochrome c (cyt c)-induced apoptosis (25). Because the presence of cyt c in the cytosol is highly proapoptotic, only cells capable of exporting antigen into the cytosol will undergo apoptosis on exposure to exogenous cyt c. Horse cyt c interacts with cytosolic Apaf-1, a component of the apoptosome required for caspase 9 activation, whereas yeast cyt c is inactive and was used here as a negative control. Surprisingly, γδ T-APCs incubated with increasing concentrations of horse cyt c induced substantial apoptosis, whereas yeast cyt c did not raise the level of

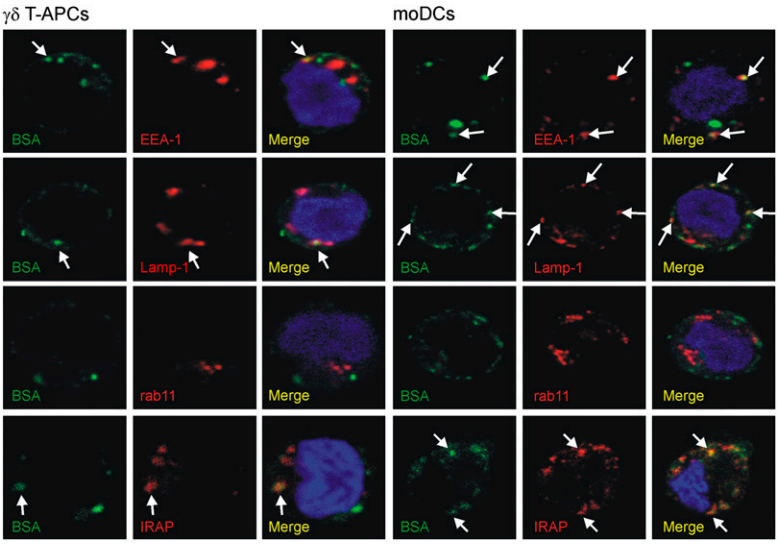

Fig. 2. Endocytosed BSA is transferred from early to late endosomes/lysosomes in γδ T-APCs and moDCs. Cells were pulsed for 1 h with BSA (green) and analyzed by confocal microscopy using the markers EEA-1, IRAP, Lamp-1, and rab11 (red) to identify early endosomes, late endosomes and lysosomes, and recycling endosomes, respectively. Nuclei are shown in blue. Examples of colocalizing vesicles are marked with arrows. Original magnification, 600×. Confocal images of selected single *z*-planes are shown, representing the analysis of 12–31 cells (30–40 *z*-planes/each) from two or three independent experiments.

apoptotic cells above the culture medium control (Fig. 3*A* and Fig. S6*A*). The addition of the caspase inhibitor Z-VAD-FMK fully inhibited apoptosis, confirming the proapoptotic function of horse cyt c (Fig. 3*A* and Fig. S6*A*). In clear contrast, no apoptosis induction was seen in moDCs (Fig. 3*B*). To extend our investigation on human DCs, we turned to physiologically more relevant DC subsets present in peripheral blood. Neither conventional DCs (lin$^-$, HLA-DR$^+$, CD1c$^+$) nor plasmacytoid DCs (lin$^-$, HLA-DR$^+$, CD304$^+$) demonstrated enhanced apoptosis in response to horse cyt c (Fig. 3*B*). In addition, no other human cell type that we analyzed (fresh and activated αβ T cells, B cells, monocytes) showed clear evidence of apoptosis induction (Fig. S6*B*). In control experiments, mouse CD8$^+$ DCs, but not CD8$^-$ DCs, were sensitive to horse cyt c treatment, in agreement with the findings of Lin et al. (25). Collectively, we report a remarkable efficiency of γδ T-APCs to translocate exogenous soluble antigen from endosomes into the cytosol, which was not seen in human in vitro or blood-derived DCs.

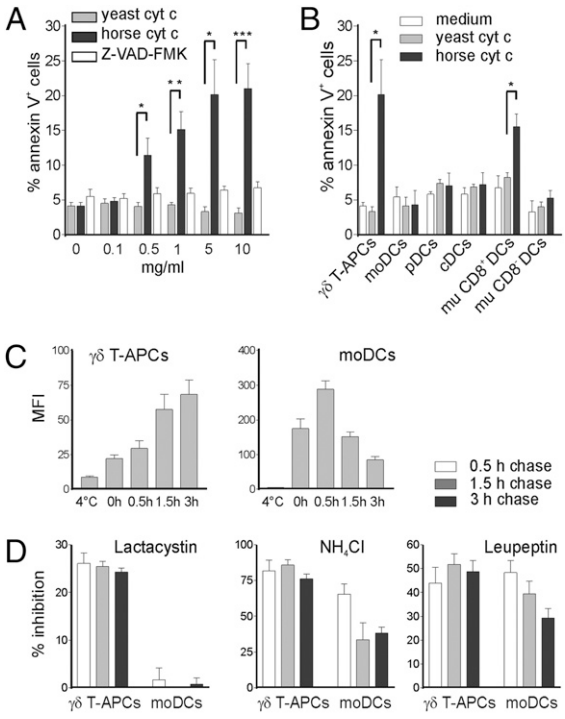

Fig. 3. γδ T-APCs, but not moDCs, export internalized protein into the cytosol for degradation by the proteasome. (*A*) γδ T-APCs were cultured for 6 h with cyt c with or without the caspase inhibitor Z-VAD-FMK. Results are expressed as percentage of apoptotic annexin V$^+$ cells (mean ± SEM; $n = 4$–6). (*B*) Apoptosis induction on incubation with 5 mg/mL of cyt c in human γδ T-APCs, moDCs, plasmacytoid DCs (pDCs), conventional DCs (cDCs), and murine (mu) spleen CD8$^+$ and CD8$^-$ DCs, expressed as percentage of annexin V$^+$ cells (mean ± SEM; $n = 3$–6). $^*P < 0.05$; $^{**}P < 0.01$; $^{***}P < 0.005$. (*C*) Mean fluorescence intensity (MFI) of cells pulsed for 30 min with DQ-BSA and chased for up to 3 h, presented as mean ± SEM ($n = 9$). (*D*) Inhibition of protein degradation in DQ-BSA–pulsed cells by lactacystin, NH_4Cl, and leupeptin over a 3 h chase period. Results are expressed as mean ± SEM from three to five independent experiments.

We next analyzed the involvement of the proteasome in antigen degradation. γδ T-APCs and moDCs were pulsed for 1 h with FITC-BSA and chased for 24 h in the presence of the proteasome inhibitor lactacystin before analysis by FACS and Western blot. The cytosolic pH is neutral, allowing the study of cytosolic FITC-BSA without interference from the acidic endosomal/lysosomal compartment, in which the FITC fluorescence is quenched. While increasing concentrations of lactacystin increased the residual fluorescence in γδ T-APCs, no difference was detected in moDCs (Fig. S7*A*). Correspondingly, protein degradation was significantly delayed by lactacystin in γδ T-APCs, but not in moDCs (Fig. S7*B*). To more accurately examine the relative contribution of the proteasome versus the lysosome to antigen degradation, we pulsed APCs with the self-quenched form of DQ-BSA, which releases its pH-independent fluorescence only after protein degradation. Confirming the delay in FITC-BSA degradation (Fig. 1*C*), γδ T-APCs continued to release fluorescent degradation products for up to 3 h after the pulse when DQ-BSA was washed away (Fig. 3*C*). In contrast, moDCs degraded most of the BSA during the pulse and the first 30 min chase period. Rapid decline of the fluorescent signal in moDCs during the chase period might be due to fluorochrome instability or excretion. While the proteasome inhibitor lactacystin did not affect antigen degradation in moDCs, it inhibited about 25% of the proteolysis in γδ T-APCs (Fig. 3*D*). In addition, the acidification inhibitor NH_4Cl and the protease inhibitor leupeptin reduced BSA degradation to a similar extend in both APCs (Fig. 3*D*). We conclude that the main contribution to proteolysis was provided by endosomal/lysosomal compartments in both APCs; however, in clear contrast to the situation in moDCs, a substantial portion of internalized antigen in γδ T-APCs was exported to the cytosol and degraded by the proteasome.

γδ T-APCs Take Up and Cross-Present Virus-Infected Cellular Debris and Virions. Up to this point, we limited our analysis to soluble antigen. γδ T-APCs were not able to take up particulate antigen,

such as bacteria, zymosan, or beads, which clearly distinguishes these APCs from phagocytes, including moDCs. However, our analysis of the uptake of fluorescently labeled cellular debris from necrotic cells found that γδ T-APCs ingested particles, as demonstrated by confocal microscopy (Fig. 4*A*). We next investigated whether γδ T-APCs were able to cross-present antigen derived from cellular debris. We incubated γδ T-APCs with debris generated from influenza virus–infected cells, and studied cross-presentation of the influenza matrix protein M1-derived immunodominant peptide M1p58-66 using HLA-A2–restricted, M1p58-66–specific $CD8^+$ T cells as responder cells (10). The functional readout included IFN-γ production in M1p58-66 tetramer–positive responder cells after coculture with APCs. In contrast to debris from noninfected cells, γδ T-APCs incubated with influenza-infected cellular debris induced strong $CD8^+$ T cell responses (Fig. 4*B*). Responder cells did not become directly activated by debris from influenza-infected cells. Cellular debris was UV irradiated and did not contain live virus, excluding a potential complication by virus infection in our system (see below). We next explored the ability of debris-treated γδ T-APCs to induce proliferation in primary blood $CD8^+$ T cells. γδ T-APCs loaded with debris from influenza-infected cells, but not uninfected cells, led to strong proliferation of M1-specific $CD8^+$ T cells (Fig. 4*C*).

To determine whether γδ T-APCs cross-presented free virus particles, we incubated cells with increasing concentrations of influenza virus, washed the cells, and then incubated them with M1p58-66–specific $CD8^+$ T cells. Remarkably, γδ T-APCs loaded with small quantities of live virus induced robust IFN-γ responses (Fig. 5*A*). Similar to debris-loaded γδ T-APCs (Fig. 4), M1-specific primary $CD8^+$ T cell responses were observed when γδ T-APCs were incubated with influenza virus alone (Fig. 5*B*). Of note, M1p58-66–specific T cell responses were inhibited by lactacystin, indicating involvement of the proteasome in the processing of influenza virus, as was seen previously with purified M1 protein (Fig. 5*C*) (10). In contrast to cells permissive to influenza infection, such as monocytes and moDCs, we did not detect viral protein synthesis (matrix protein M1 and nucleoprotein NP) in γδ T-APCs during incubation with live virus (Fig. S8 *A* and *B*). Moreover, UV- and heat-inactivated (56 °C) virus largely retained its ability to induce M1-specific $CD8^+$ T cell responses (Fig. 5*C*). In contrast,

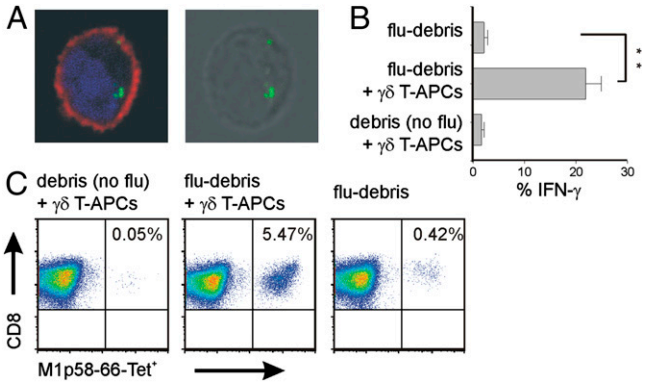

Fig. 4. γδ T-APCs take up and cross-present cellular debris. (*A*) γδ T-APCs (red) were incubated with debris (green), stained with the nuclear dye DRAQ5 (blue), and analyzed by confocal microscopy. A single section in the middle of the cell is shown. Original magnification, 600×. Pictures are representative of two independent experiments. (*B*) γδ T-APCs were incubated with debris from influenza-infected cells (flu-debris) and cocultured with M1p58-66–specific $CD8^+$ T cells. Results are expressed as percentage of IFN-γ–producing cells, gated on M1p58-66 Tet^+ cells (mean ± SEM, $n = 4$). $^{**}P = 0.0054$. (*C*) Blood $CD8^+$ T cells were cocultured with debris-loaded γδ T-APCs, and M1p58-66 Tet^+ cells were quantified after 11 days. One of two independent experiments is shown. Negative controls included debris from noninfected cells [debris (no flu)] and infected debris without γδ T-APCs.

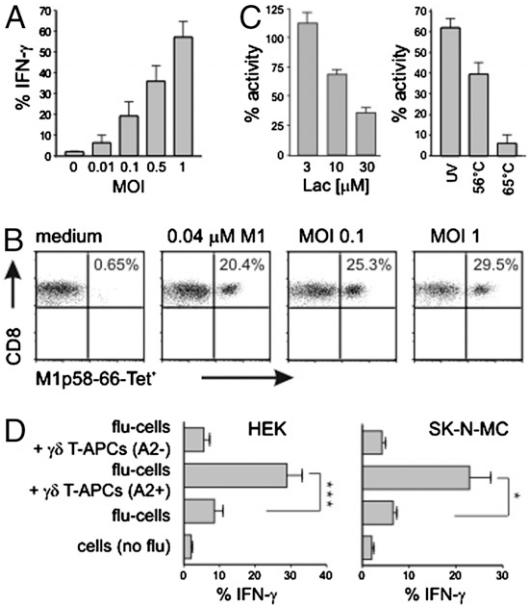

Fig. 5. γδ T-APCs cross-present live and inactivated virus. (*A*) Percentage of IFN-γ–producing M1p58-66 Tet^+ T cells in response to γδ T-APCs incubated with increasing concentrations of live influenza virus. Results are expressed as mean ± SEM from three to seven independent experiments. (*B*) Blood $CD8^+$ T cells were cocultured with virus-treated γδ T-APCs, and M1p58-66 Tet^+ cells were quantified by FACS after 11 days. Controls included medium and M1 protein–loaded γδ T-APCs. One of three independent experiments is shown. (*C*) Residual efficiency of γδ T-APCs to cross-present virus (MOI 1) in the IFN-γ responder cell assay after pretreatment of γδ T-APCs with lactacystin (*Left*) or after processing of UV or heat-inactivated virus (*Right*). Data are presented as percentage of activity (mean ± SEM; $n = 4$–5). (*D*) Influenza-infected cells (flu-cells) were incubated with γδ T-APCs for 18 h, and cross-presentation was assessed as IFN-γ production by M1p58-66–specific $CD8^+$ T cells (mean ± SEM; $n = 4$–7). Negative controls included noninfected cells (no flu), HLA-$A2^-$ γδ T-APCs, and virus-infected cells in the absence of γδ T-APCs. $^{*}P = 0.015$; $^{***}P = 0.0018$.

the response was abolished if the virus was heat-inactivated at 65 °C, a temperature that caused the denaturation of influenza hemagglutinin, which controls fusion of the viral nucleocapsid with endosomes and subsequent viral delivery into the cytosol. It was reported previously that DCs loaded with inactivated influenza virus elicited CTL responses only if the virus retained its fusogenic activity (26). To mimic physiological conditions, γδ T-APCs were incubated with virus-infected live cells before culture with $CD8^+$ responder T cells. Even though HEK293 cells are HLA-$A2^+$ and thus potentially able to directly present viral antigen, $CD8^+$ T cell responses to influenza-infected HEK293 cells were low. The responses were increased substantially when HLA-$A2^+$ γδ T-APCs were added, however (Fig. 5*D*). In agreement with the requirement for HLA-$A2^+$ APCs, only background responses were seen when HLA-$A2^-$ γδ T-APCs were used. These results were confirmed in experiments using the HLA-$A2^-$ cell line SK-N-MC as a virus source (Fig. 5*D*). Collectively, these experiments demonstrate that γδ T-APCs are fully capable of cross-presenting cellular debris and virus particles for induction of strong anti-influenza CTL responses.

Discussion

Although γδ T cells with APC functions have been described in several species, the most advanced studies have been performed with human γδ T cells (10, 12, 13, 27–29). Interestingly, human γδ T-APCs were particularly effective at cross-presenting soluble protein to $CD8^+$ T cells (10). The process of cross-presentation is of paramount importance for the induction of CTL responses against tumors or virus-infected cells (1–4). For lack of a better alternative, moDCs have been widely used in experimental immunotherapy settings, but the success

rates generally have been low (30). While the expert phagocytic properties and processing of particulate antigen is well known in moDCs (20, 31), the cross-presentation of soluble protein is inefficient (7, 9–11). In contrast, the ease of manipulation of human γδ T-APCs and these cells' expert ability to cross-present soluble protein make them a promising new tool for immunotherapy. The mechanisms underlying cross-presentation in γδ T-APCs remain unknown, however. In the present study, we have demonstrated that γδ T-APCs differ fundamentally from moDCs in their ability to process internalized antigen for loading onto MHC I and presentation to $CD8^+$ T cells.

First, we found that antigen degradation occurred much more slowly in γδ T-APCs than in moDCs. In agreement with this, the endosomal pH in moDCs dropped to 4.0 within 3 h after endocytosis, indicating rapid access of internalized antigen to lysosomal proteases. In stark contrast, in γδ T-APCs, the pH in BSA-containing endosomes increased by one increment, to 7.0, during the first 3 h chase period, before returning to 6.0. In DCs, an increased dwell time in endosomes, controlled by a delay in acidification, is known to favor antigen cross-presentation (20–22, 31). Our findings may be unexpected in the light of reports showing that protein degradation occurs much slower in DCs compared to macrophages (21). However, several DC studies have also shown that macropinocytosis of soluble protein leads to faster lysosomal proteolysis than receptor-mediated antigen uptake (32, 33).

Second, γδ T-APCs readily translocated exogenous antigen into the cytosol, as demonstrated by cyt c–induced apoptosis and proteasome inhibition studies. Using exogenous cyt c, Lin et al. (25) highlighted the superior cross-presenting function of murine $CD8^+$ DCs. Taking advantage of this experimental approach, we demonstrated that γδ T-APCs outperformed moDCs in the translocation of cyt c into the cytosol. In fact, both moDCs and human blood DCs were insensitive to the cyt c treatment, indicating that the "true" cross-presenting DCs might be found in human tissues. This surprising finding further underscores the efficient vesicular proteolysis in moDCs that overrides cross-presentation of external soluble antigen. In support of this, inhibition of the proteasome did not affect protein degradation in moDCs, whereas inhibition of lysosomal proteolysis was very effective. In contrast, in γδ T-APCs, proteasome inhibition caused a substantial reduction in antigen processing and overall protein degradation.

Third, our confocal microscopy studies did not reveal a distinct vesicular compartment in γδ T-APCs that could contribute to cross-presentation. Internalized antigen colocalized with early endosomes and within 1.5 h relocated to late endosomes or lysosomes, in line with the prominent contribution of this compartment to protein degradation. While we did not detect antigen in recycling endosomes in either APC, we found endocytosed protein within vesicles harboring the aminopeptidase IRAP, which was recently shown to participate in a vesicular, yet proteasome-dependent, cross-presentation pathway (24). Collectively, our data indicate a mechanism for the expert cross-presentation capacity of γδ T-APCs that involves delayed antigen processing and efficient translocation into the cytosol. In contrast, we have no evidence for a dominant role of the cytosolic pathway in moDCs.

moDCs outperformed γδ T-APCs in the uptake of beads and bacteria, indicating poor phagocytic properties. These findings contradict a recent report published during the preparation of this manuscript (14). However, we showed that γδ T-APCs were able to take up and cross-present cellular debris. Of interest, γδ T-APCs were very efficient in processing influenza virus, triggering $CD8^+$ T cell responses after incubation with viruses at multiplicity of infection (MOI) of <0.1. In clear contrast to moDCs, monocytes, and diverse epithelial cell lines, γδ T-APCs were not productively infected by influenza virus, and inactivated particles were similarly active as substrates for antigen processing, thus ruling out the classical (endogenous) pathway of MHC I presentation.

How do our findings fit with the involvement of γδ T cells in antimicrobial and antitumor immunity? Accumulating evidence supports the view of a first-line defense of γδ T cells in antimicrobial immunity, mediated by rapid release of cytokines and lysis of infected target cells (15, 34). More recent data portray γδ T cells as controllers of adaptive immunity by bridging the early phase of innate immune response with the late-phase, antigen-specific T and B cell responses (15, 18, 34). Human blood Vγ9Vδ2 T cells respond broadly to HMB-PP, which is specifically produced by microbes. The kinetics and magnitude of γδ T cell responses to HMB-PP both in vitro and in infected individuals are astounding (16, 18). An equivalent subset of Vγ9Vδ2 T cells is absent in mice, and although murine γδ T cells are known to participate in antimicrobial immune defense, we have little knowledge about the antigen(s) to which they respond (15). Vγ9Vδ2 T cells also become engaged in antitumor immunity through recognition of stress markers or certain metabolites, and play a role in antiviral immunity (35). They often are found in increased numbers in viral infections such as HIV, influenza, or herpes simplex virus 1 and are thought to recognize virus-infected cells via stress-inducible molecules, virus-induced phosphoantigens, or heat-shock proteins (35, 36). Of interest for the present study, human γδ T cells efficiently kill influenza-infected macrophages (37).

The following working hypothesis combines the innate properties of Vγ9Vδ2 T cells with their ability to present antigen. Circulating Vγ9Vδ2 T cells express inflammatory chemokine receptors, allowing their immediate recruitment to sites of infection (38), were they become activated and turn into γδ T-APCs. They then lyse affected target cells and liberate antigen for subsequent uptake, processing, and antigen presentation. A change in their migratory properties allows the homing of $CCR7^+$ γδ T-APCs to draining lymph nodes, where they trigger microbe- (or tumor-) specific $CD4^+$ and $CD8^+$ αβ T cell responses (10, 12, 38). This model emphasizes the rapid innate-like response of human Vγ9Vδ2 T cells to microbial antigens and to tumor cells, as well as the contribution of γδ T-APCs to the early phase of adaptive immunity.

Materials and Methods

Cell Isolation and Culture. Peripheral blood mononuclear cells (PBMCs) were isolated from healthy donors using Lymphoprep (Axis-Shield), according to the local ethical guidelines on experimentation with human samples. Vγ9Vδ2 T cells (96%–99% pure) were isolated using Vδ2-PE or Vγ9-PE-Cy5 and anti-PE microbeads or, for confocal microscopy, anti-TCR-γδ-biotin. γδ T cell lines (80–90% pure) were generated from PBMCs stimulated with synthetic HMB-PP (kindly provided by H. Jomaa, Giessen, Germany) and cultured for 3 weeks with 20 U/mL of IL-2 (Proleukin; Chiron). γδ T-APCs were generated from purified γδ T cells via stimulation for 18–48 h with 20–50 nM HMB-PP, 20–50 U/mL IL-2, and 70-Gy–irradiated HLA-$A2^-$ EBV-transformed B cells at a γδ:feeder cell ratio of 5:1. Occasionally, γδ T cell lines were used with similar results. αβ T cells were purified using the Miltenyi Pan T Cell Isolation Kit and stimulated for 2 days with 1 μg/mL of PHA (Sigma-Aldrich). MoDCs were derived from monocytes purified with CD14 microbeads (Miltenyi) and cultured for 6–7 days with 50 ng/mL of GM-CSF and 10 ng/mL of IL-4 (Peprotech). Blood DCs were enriched from PBMCs by depleting lin^+ cells (CD3, CD14, CD19, and CD56). Spleen DCs from C57BL/6 mice were purified using CD11c microbeads (Miltenyi).

Endocytosis. Cells were pulsed for 0.5–1 h with 1 mg/mL of FITC-BSA, Alexa Fluor 488-BSA, or Alexa Fluor 647-BSA or with 0.5 mg/mL of DQ-BSA (all from Invitrogen) and washed extensively before the chase period. In some experiments, cells were preincubated for 30 min with 5 μM cytochalasin D (Sigma-Aldrich), 250 μM DMA (Sigma-Aldrich), 50 mM NH_4Cl, 100 μM leupeptin, 10 μM diphenylene iodonium, and 20 μM Z-VAD-FMK or 1–10 μM lactacystin (Alexis). Inhibitors were kept in the medium throughout the chase period. The percent inhibition was calculated as the reduction in geometric MFI of inhibitor-treated cells versus untreated cells after background fluorescence (4 °C) was subtracted. Cells incubated for 6 h with cyt c (Sigma-Aldrich) were stained with annexin V (BD Biosciences). Debris was generated by repetitive freezing-thawing of virus-infected MDCK cells or the PKH26 (Sigma-Aldrich)-labeled cell line RAW264.7.

Influenza A Virus Infection. Cells were infected for 2 h with influenza A strain A/PR8/34 (PR8) virus (MOI 0.5–3; kindly provided by A. Gallimore, Cardiff, United Kingdom) in serum-free medium and cultured for 24 h. Replication-deficient virus was generated by UV inactivation for 30 min at a distance of 5 cm or by heating for 30 min. Virus inactivation was confirmed by standard plaque-forming unit assay.

Antigen Presentation Assays. M1-specific $CD8^+$ T cells were generated by stimulating PBMCs with 0.1 nM M1p58-66 peptide (kindly provided by P. Romero, Lausanne, Switzerland). After 3 days, 40 U/mL of IL-2 was added. Cells were restimulated after 10–14 days in the presence of irradiated (40 Gy) PBMCs. Resting cells with 25–45% M1p58-66–specific cells were used for assays, as determined by tetramer staining (kindly provided by A. Sewell, Cardiff, United Kingdom). Recombinant influenza M1 protein (kindly provided by M. Luo, Birmingham, AL), virus, or debris was added to γδ T-APCs for 18 h. The APCs were washed extensively before culture with responder cells at an APC to responder cell ratio of 1:2–3:1. Brefeldin A (10 μg/mL; Sigma-Aldrich) was added after 45 min; 5 h later, intracellular IFN-γ was measured by gating on CD8 and M1p58-66 tetramer–positive cells. For primary T cell stimulation, $CD8^+$ T cells were cocultured with antigen-loaded and irradiated (12 Gy) γδ T-APCs at an APC to responder cell ratio of 1:10. Twenty units per milliliter IL-2 was added on day 3, and tetramer-positive cells were analyzed on day 11.

pH Measurement. pH was measured as described previously (39). In brief, cells were incubated for 1 h with 1 mg/mL of FITC-BSA and Alexa Fluor 647-BSA, chased, and analyzed by FACS. The FL1:FL4 ratio was calculated, and pH values were extrapolated from calibration curves obtained from the same batch of cells incubated for 4 min in buffers (pH 5–8) in the presence of 10 μM monensin and nigericin (Sigma-Aldrich).

Western Blot Analysis. Equal numbers of cells were lysed in sample buffer, sonicated, and run on a 12.5% SDS-PAGE gel. Gels were blotted on a nitrocellulose membrane and stained with anti-FITC or β-actin antibodies. Blots were developed using ECL Western blotting substrate (Pierce) and captured on radiographic film (GE Healthcare). Densitometric analysis of scanned autoradiographs was done using ImageJ software.

Confocal Microscopy. FITC-BSA–, Alexa Fluor 488-BSA–, or Alexa Fluor 647-BSA–loaded cells were fixed in formaldehyde, permeabilized with 0.1% saponin, and stained for EEA-1, Lamp-1, rab11, or IRAP. Cells were incubated with Alexa Fluor 488– or Alexa Fluor 549–labeled secondary antibodies (Invitrogen), followed by the nuclear stain DRAQ5 (Axxora) or Sytox Orange (Invitrogen). For simplicity, nuclear stains were false-colored in blue, endocytosed BSA was colored in green, and vesicular stains were colored in red. Before endocytosis of cellular debris, γδ T-APCs were surface-stained with PKH67 (Sigma-Aldrich) in accordance with the supplier's protocol. Cells were mounted using Prolong Gold (Invitrogen). Images were acquired by scanning in sequential mode on a Leica LSM TCS SP5 confocal microscope (1.4 NP Plan Apochromat) and processed with Imaris 6.1.3 (Bitplane). Quantitative colocalization was performed using the ImarisColoc module and the automatic threshold function.

Statistical Analysis. Data are expressed as mean ± SEM and analyzed using the two-tailed unpaired Student *t* test, with differences considered significant as indicated in the figures: $*P < 0.05$; $**P < 0.01$; and $***P < 0.005$.

The media, reagents, and antibodies used are described in *SI Materials and Methods*.

ACKNOWLEDGMENTS. We thank A. Sewell and E. Edwards (Cardiff, United Kingdom) for providing tetramers, A. Gallimore and S. Lauder (Cardiff, United Kingdom) for providing influenza virus and plaque forming unit assays, P. van Endert (Paris, France) for providing anti-IRAP antibody, H. Jomaa (Giessen, Germany) for providing synthetic HMB-PP, P. Romero (Lausanne, Switzerland) for providing M1p58-66 peptide, and M. Luo (Birmingham, AL) for providing recombinant influenza M1 protein. This work was supported by a grant from the European Sixth Framework Programme to the INNOCHEM consortium. M. E. is the recipient of a Wellcome Trust 'Value in People' Award and a Research Councils UK Fellowship in Translational Research. B.M. is the recipient of a Royal Society Wolfson Research Merit Award.

1. Cresswell P, Ackerman AL, Giodini A, Peaper DR, Wearsch PA (2005) Mechanisms of MHC class I–restricted antigen processing and cross-presentation. *Immunol Rev* 207: 145–157.
2. Lin ML, Zhan Y, Villadangos JA, Lew AM (2008) The cell biology of cross-presentation and the role of dendritic cell subsets. *Immunol Cell Biol* 86:353–362.
3. Villadangos JA, Schnorrer P (2007) Intrinsic and cooperative antigen-presenting functions of dendritic-cell subsets in vivo. *Nat Rev Immunol* 7:543–555.
4. Vyas JM, Van der Veen AG, Ploegh HL (2008) The known unknowns of antigen processing and presentation. *Nat Rev Immunol* 8:607–618.
5. Di Pucchio T, et al. (2008) Direct proteasome-independent cross-presentation of viral antigen by plasmacytoid dendritic cells on major histocompatibility complex class I. *Nat Immunol* 9:551–557.
6. Hoeffel G, et al. (2007) Antigen crosspresentation by human plasmacytoid dendritic cells. *Immunity* 27:481–492.
7. Schnurr M, et al. (2005) Tumor antigen processing and presentation depend critically on dendritic cell type and the mode of antigen delivery. *Blood* 105:2465–2472.
8. Villadangos JA, Young L (2008) Antigen-presentation properties of plasmacytoid dendritic cells. *Immunity* 29:352–361.
9. Nagata Y, et al. (2002) Differential presentation of a soluble exogenous tumor antigen, NY-ESO-1, by distinct human dendritic cell populations. *Proc Natl Acad Sci USA* 99:10629–10634.
10. Brandes M, et al. (2009) Cross-presenting human gammadelta T cells induce robust $CD8^+$ alphabeta T cell responses. *Proc Natl Acad Sci USA* 106:2307–2312.
11. Schnurr M, et al. (2009) ISCOMATRIX adjuvant induces efficient cross-presentation of tumor antigen by dendritic cells via rapid cytosolic antigen delivery and processing via tripeptidyl peptidase II. *J Immunol* 182:1253–1259.
12. Brandes M, Willimann K, Moser B (2005) Professional antigen-presentation function by human gammadelta T cells. *Science* 309:264–268.
13. Landmeier S, et al. (2009) Activated human gammadelta T cells as stimulators of specific $CD8^+$ T-cell responses to subdominant Epstein-Barr virus epitopes: Potential for immunotherapy of cancer. *J Immunother* 32:310–321.
14. Wu Y, et al. (2009) Human γδ T cells: A lymphoid lineage cell capable of professional phagocytosis. *J Immunol* 183:5622–5629.
15. Hayday AC (2009) Gammadelta T cells and the lymphoid stress-surveillance response. *Immunity* 31:184–196.
16. Morita CT, Jin C, Sarikonda G, Wang H (2007) Nonpeptide antigens, presentation mechanisms, and immunological memory of human Vgamma2Vdelta2 T cells: Discriminating friend from foe through the recognition of prenyl pyrophosphate antigens. *Immunol Rev* 215:59–76.
17. Carding SR, Egan PJ (2002) Gammadelta T cells: Functional plasticity and heterogeneity. *Nat Rev Immunol* 2:336–345.
18. Moser B, Eberl M (2007) Gammadelta T cells: Novel initiators of adaptive immunity. *Immunol Rev* 215:89–102.
19. Schnorrer P, et al. (2006) The dominant role of $CD8^+$ dendritic cells in cross-presentation is not dictated by antigen capture. *Proc Natl Acad Sci USA* 103:10729–10734.
20. Trombetta ES, Mellman I (2005) Cell biology of antigen processing in vitro and in vivo. *Annu Rev Immunol* 23:975–1028.
21. Delamarre L, Pack M, Chang H, Mellman I, Trombetta ES (2005) Differential lysosomal proteolysis in antigen-presenting cells determines antigen fate. *Science* 307:1630–1634.
22. Savina A, et al. (2006) NOX2 controls phagosomal pH to regulate antigen processing during crosspresentation by dendritic cells. *Cell* 126:205–218.
23. Monu N, Trombetta ES (2007) Cross-talk between the endocytic pathway and the endoplasmic reticulum in cross-presentation by MHC class I molecules. *Curr Opin Immunol* 19:66–72.
24. Saveanu L, et al. (2009) IRAP identifies an endosomal compartment required for MHC class I cross-presentation. *Science* 325:213–217.
25. Lin ML, et al. (2008) Selective suicide of cross-presenting $CD8^+$ dendritic cells by cytochrome c injection shows functional heterogeneity within this subset. *Proc Natl Acad Sci USA* 105:3029–3034.
26. Bender A, Bui LK, Feldman MA, Larsson M, Bhardwaj N (1995) Inactivated influenza virus, when presented on dendritic cells, elicits human $CD8^+$ cytolytic T cell responses. *J Exp Med* 182:1663–1671.
27. Cheng L, et al. (2008) Mouse γδ T cells are capable of expressing MHC class II molecules, and of functioning as antigen-presenting cells. *J Neuroimmunol* 203:3–11.
28. Takamatsu HH, Denyer MS, Wileman TE (2002) A sub-population of circulating porcine gammadelta T cells can act as professional antigen-presenting cells. *Vet Immunol Immunopathol* 87:223–224.
29. Collins RA, et al. (1998) Gammadelta T cells present antigen to $CD4^+$ alphabeta T cells. *J Leukoc Biol* 63:707–714.
30. Steinman RM, Banchereau J (2007) Taking dendritic cells into medicine. *Nature* 449: 419–426.
31. Savina A, Amigorena S (2007) Phagocytosis and antigen presentation in dendritic cells. *Immunol Rev* 219:143–156.
32. van Montfoort N, et al. (2009) Antigen storage compartments in mature dendritic cells facilitate prolonged cytotoxic T lymphocyte cross-priming capacity. *Proc Natl Acad Sci USA* 106:6730–6735.
33. Shen H, et al. (2006) Enhanced and prolonged cross-presentation following endosomal escape of exogenous antigens encapsulated in biodegradable nanoparticles. *Immunology* 117:78–88.
34. Holtmeier W, Kabelitz D (2005) Gammadelta T cells link innate and adaptive immune responses. *Chem Immunol Allergy* 86:151–183.
35. Poccia F, et al. (2005) Antiviral reactivities of gammadelta T cells. *Microbes Infect* 7: 518–528.
36. Shao L, et al. (2009) Expansion, re-expansion and recall-like expansion of Vγ2Vδ2 T cells with enhanced effector function in smallpox vaccination and monkeypox virus infection. *J Virol* 83:11959–11965.
37. Qin G, et al. (2009) Phosphoantigen-expanded human γδ T cells display potent cytotoxicity against monocyte-derived macrophages infected with human and avian influenza viruses. *J Infect Dis* 200:858–865.
38. Brandes M, et al. (2003) Flexible migration program regulates γδ T-cell involvement in humoral immunity. *Blood* 102:3693–3701.
39. Altan N, Chen Y, Schindler M, Simon SM (1998) Defective acidification in human breast tumor cells and implications for chemotherapy. *J Exp Med* 187:1583–1598.